

Spectroscopic constraints on growth of Siberian mixed-habit diamonds

Sergei Yu. Skuzovtov^{1,2} · Dmitry A. Zedgenizov^{2,3} · Alexander L. Rakevich⁴

Received: 27 October 2016 / Accepted: 26 April 2017 / Published online: 23 May 2017
© Springer-Verlag Berlin Heidelberg 2017

Abstract Notable within-crystal variability of mineralogical and geochemical properties of single natural diamonds are commonly attributed to changing chemistry of parental fluids, sources of carbon and redox conditions of diamond precipitation. A distinct type of compositional heterogeneity (mixed-habit structure) is well-known to occur in diamonds as well as in many other minerals due to purely “structural” reasons that are unequal crystal chemistry of crystallographically different faces and selective absorption and fractionation of impurities between adjacent growth pyramids. Based on the combined cathodoluminescence, Fourier-transformed infrared spectroscopy and photoluminescence spectroscopy, study of nine diamond crystals with different growth histories and external morphology, but all showing mixed-habit patterns at different growth stages, we show that mixed-diamonds may grow in closed system conditions or with a slowly decreasing growth rate from a media with a much lower impurity content than previously thought. Intracrystal nitrogen distribution seems to be a function of growth rate even in the cases of unusual

impurity partitioning between growth sectors. Generally poor with IR-active hydrogen at moderate nitrogen aggregation parameters, studied diamonds likely resemble the low hydrogen content from the growth medium that, for cubic diamonds, was typically suggested hydrogen-rich and a crucial factor for growth of cubic and mixed-habit diamonds. We also show that mixed-habit diamond growth may occur not only in peridotitic suite but also in an extended field of geochemical affinities from high-Ni to low-Ni or maybe even Ni-free environments, such as pyroxenitic or eclogitic.

Keywords Siberian craton · Diamond · Mixed-habit growth · Nitrogen · Hydrogen · Infrared absorption · Photoluminescence

Introduction

Natural diamonds are well known to exhibit two principle growth morphologies—octahedron and cuboid (near-cube crystal shape often with the fibrous internal structure) (Orlov 1977). Based on the crystal growth fundamentals, the stability of flat octahedron faces and rough hummocky cuboid surfaces and—therefore—their proportion in the overall diamond habit are controlled by the carbon saturation of the growth medium (Sunagawa 1984, 1990). In case of the low oversaturation degree, layered growth of monocrystalline octahedral diamonds occurs, whereas high degrees of oversaturation lead to high-rate skeletal and fibrous growth. This evident link between the growth morphology and fluid/melt saturation easily controlled by a changing temperature resulted in a long-lasting suggestion of a high-T origin of octahedral diamonds and—on the other hand—relatively low-T nature of cubic stones (e.g.

Communicated by Timothy L. Grove.

✉ Sergei Yu. Skuzovtov
skuzovtov@igc.irk.ru

¹ Vinogradov Institute of Geochemistry, Russian Academy of Sciences, Siberian Branch, 1A, Favorskogo Str., Irkutsk 664033, Russian Federation

² Novosibirsk State University, Novosibirsk 630090, Russia

³ Sobolev Institute of Geology and Mineralogy, Russian Academy of Sciences, Siberian Branch, Novosibirsk 630090, Russia

⁴ Institute of Laser Physics (Irkutsk Department), Russian Academy of Sciences, Siberian Branch, Irkutsk 664033, Russia

Haggerty 1986). Beside the saturation characteristics, diamond growth mechanism and resulting morphology may be influenced by the physical state of the growth medium, e.g. its viscosity that may control the rate of carbon diffusion through a fluid/melt to a growing crystal surface and—therefore—stability or instability of octahedron faces (Bulanova et al. 1993). As revealed by a few experimental studies in metal–carbon, diamond nucleation, growth rate and morphology as well as the other diamond properties may be directly influenced by concentration of additives (e.g. nitrogen or water) in a diamond-forming liquid (Palyanov et al. 2010, 2013; Khokhryakov et al. 2015). However, the application of the latter to natural diamond-systems and natural gem-quality diamonds is quite strict due to commonly lacking independent indicators of P–T–fO₂ growth conditions and parental media as well as due to an uncertain behaviour of abundant impurities relative to a growing diamond (e.g. see Mikhail and Howell 2016 for review on nitrogen).

Regardless of really acting reasons for morphology variations, it is undisputed that a change of growth conditions (pressure, temperature, degree of carbon saturation, redox state) in a closed system or due to a flux of a brand-new diamond-forming fluid may result in both notable intracrystal variations of diamond properties and re-shaping of natural stones, e.g. in case of coated diamonds (Boyd et al. 1994 and references therein; Skuzovatov et al. 2012) or more seldom octahedral crystals with the microinclusion-rich cubic cores (e.g. Zedgenizov et al. 2006; Skuzovatov et al. 2011, 2015, 2016). A distinct and the most uncertain type of structural heterogeneity is observed in diamonds exhibiting a simultaneous growth of both cuboid and octahedron faces, so-called mixed-habit diamonds (Lang 1974; Suzuki and Lang 1976; Welbourn et al. 1989; Bulanova et al. 2002; Cartigny et al. 2003; Zedgenizov and Harte 2004; Lang et al. 2004, 2007; Rondeau et al. 2004; Howell et al. 2013a, b, 2015; Smit et al. 2016). According to the early studies of Seal (1965), Harrison and Tolansky (1964), Lang (1974) and Suzuki and Lang (1976), many of the diamonds commonly exhibit an early mixed-habit stage followed by “extinction” of the cube growth pyramids, as they are growing out to produce octahedral crystals. Much rarer are cubic crystals with a concentric zoning and subtle sectors of octahedron (Moore and Lang 1972). For some of natural stones, mixed-habit patterns are recognized optically through the distribution of microinclusions (Smit et al. 2016) or coloration due to specific defects (Babich and Feigelson 2009a; Howell et al. 2013a); however, for most of mixed-habit diamonds growth patterns are distinguishable only by characteristic luminescence making such samples tough for distinguishing and further studies.

Most of the studies focused on mixed-habit samples have broached a wide range of aspects of the diamond

formation, such as redox conditions (Smit et al. 2016), carbon and nitrogen isotope (e.g. Cartigny et al. 2003; Zedgenizov and Harte 2004; Howell et al. 2013a, 2015) as well as trace element (Howell et al. 2013b) fractionation between growth sectors. Along with that, the biggest challenge—to give general constrains for possible growth conditions of mixed-habit diamonds in the Earth’s mantle—still remains almost unsolved. Here we performed combined study of the internal structure (by cathodoluminescence and photoluminescence topography) and optical characteristics (FTIR and PL local spectroscopy) of a number of natural mixed-habit diamonds from Siberian kimberlites in order to reassess growth conditions, post-growth history as well as to testify the existing models providing new insights to mixed-habit growth.

Samples and methods

Nine diamond crystals with different external shapes and internal structures all from 1 to 2 mm in size were selected for the study from a large collection of kimberlitic diamonds of the Yakutian province (Siberian craton) (Fig. 1). Five diamonds (samples A1263, I-17, Ud-02-305, NBI-67, A100111) are from the Mir, Internatsionalnaya (both pipes belonging to the Malobotuobia kimberlite field), Udachnaya (Daldyn field), Nyurbinskaya (Nakyn field), and Aikhal (Alakit–Markha field), respectively. The other four (S-4, S-27, S-26, S-37) were selected from a mixed population derived from the Internatsionalnaya and Udachnaya pipe. The diamonds were polished parallel to one of the {110} surfaces into thin plates no more than 200 microns and examined by cathodoluminescence topography (CL) from both sides of the plate to check the observed internal structure, constrain the position for further spectroscopic studies and minimize possible signal contamination due to integration of signal from several distinct growth zones and/or sectors. Cathodoluminescence images were obtained using a LEO 1430VP electron scanning microscope with a beam current of 10 nA and accelerating voltage of 20 kV at the Analytical Center of Sobolev Institute of Geology and Mineralogy (Novosibirsk, Russia). The type and concentration of major nitrogen- and hydrogen-related defects were determined by Fourier-transformed IR spectroscopy. Measurements were performed using a Bruker Vertex 70 FTIR spectrometer with a HYPERION 2000 IR microscope. Absorption spectra were recorded in different diamond zones, with an aperture of 50 × 50 μm and a spectral range of 7500–750 cm⁻¹ (spectral resolution 4 cm⁻¹, cumulative signal 30 scans per spectrum). Acquired spectra have been quantified through regression-based deconvolution using a self-made Excel-based spreadsheet and SpectrExamination software (compiled and provided by

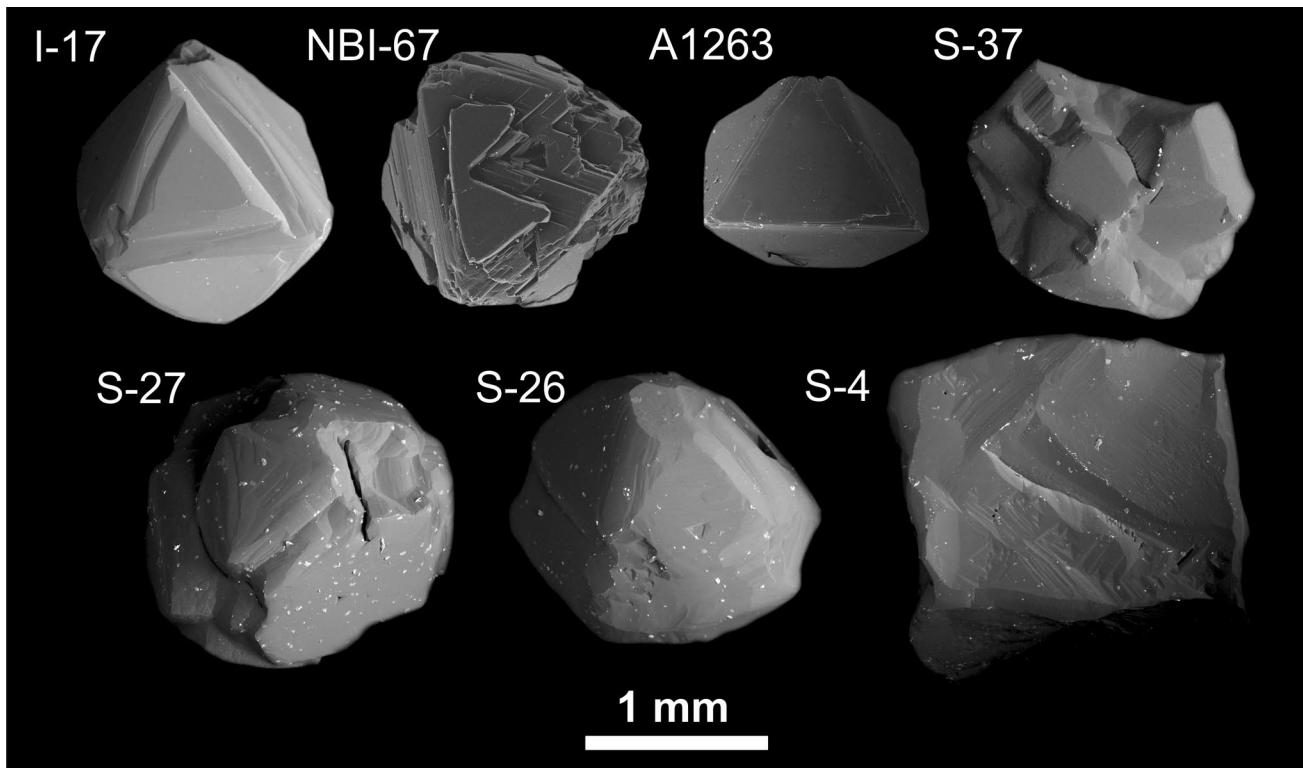


Fig. 1 SEM images of crystal morphology of seven studied diamonds (see description in the text). Presented ones are octahedrons with (I-17, NBI-67) or without (A1263) a rough but variable growth/

dissolution sculpture, cuboctahedrons (S-26, S-27 and S-37) and a cubic stone (S-4). Not shown here are two octahedrons (primitive, A100111, and coated, Ud-02-305)

Oleg Kovalchuk, NIGP Alrosa). Both procedures include baseline correction, internal standardization by the intrinsic diamond absorption, and subtraction of characteristic absorption of A, B and C-type nitrogen defects. The concentration of each defect has been estimated using ratios proposed by Boyd et al. (1995). The uncertainty of the nitrogen content calculation due to instrumental error and that of the spectra deconvolution is considered to be within 10% limit. The uncertainty for nitrogen aggregation was estimated within $\pm 3\%$ (2σ). In order to provide the fuller data for impurity distribution in a diamonds with the most complicated growth pattern (similar for A1263 and Ud-02-305 samples), the A1263 diamond has been mapped using the same instrumentation and technique. The distribution of UV fluorescence in diamonds has been studied by means of the confocal luminescence microscopy with a temporal resolution using a MicroTime 200 luminescence microscope at the Irkutsk Branch of the Institute of Laser Physics (Irkutsk, Russia). The distribution patterns for luminescence over the sample were obtained during excitation from lasers with wavelengths of 405, 450, and 532 nm; those shown further in figures are for the 532 nm excitation that gives the clearest representation of the growth patterns. The PL spectra have separately been acquired for growth

sectors of cube and octahedron in six samples showing contrast UV fluorescence patterns at the liquid nitrogen temperature (77 K) during excitation from a picosecond pulse laser with a 375-nm wavelength as previously reported by Skuzovatov et al. (2015).

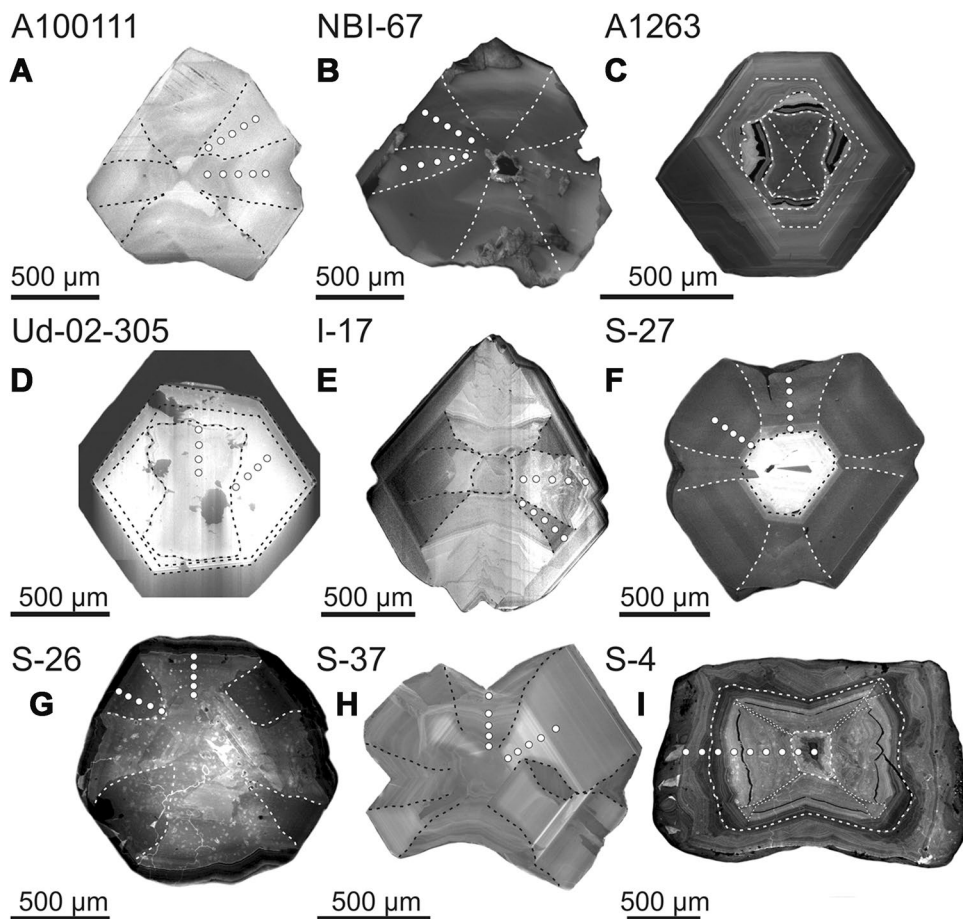
Results

Internal structures of mixed-habit diamonds (by CL topography)

Diamonds A100111 (Fig. 2a) and NBI-67 (Fig. 2b) are octahedral crystals showing mixed-habit structure in the whole crystal volume. For both samples, the octahedron/cuboid surface ratio remains almost constant throughout the crystal leading to the mixed-habit cuboctahedral zoning. At the terminal stage growth of cube sectors in A100111 is inhibited resulting in the almost pure octahedral habit with negative pits instead of $\{100\}$ surfaces delimited by (111) and $(\bar{1}\bar{1}1)$ growing faces; while NBI-67 preserves a minor cube surface in its final shape.

A1263 has a mixed-habit “hourglass” core overgrown first by hummocky (“agate-like”) cuboid surfaces and then

Fig. 2 Cathodoluminescence images of polished plates made of all studied diamond crystals. Growth sectors of octahedron and cube along with some other growth zones are *outlined*. *Filled circles* are positions of IR spectra acquisition (see below)



by an octahedral layered rim (Fig. 2c) that is very similar to diamonds reported by Bulanova et al. (2002) and Kaminsky and Khachatryan (2004). Ud-02-305 is a typical coated octahedron with a transparent “hourglass” type mixed-habit core (Fig. 2d) similar to that of A1263 and an opaque microinclusion-bearing coat. I-17 is a cloudy diamond of an overall octahedral habit (Fig. 2e) reported by Skuzovtsov et al. (2011, 2016), with a subtle microinclusion-rich cubic core surrounded by a mixed-habit intermediate zone exhibiting a clear decrease in the cube/octahedron surface ratio but clearly preserving (001) and (010) curvilinear cube sectors and a thin octahedral rim at a final stage.

Along with abundant octahedral crystals studied diamonds include samples with a higher input of {100} surfaces. Two diamonds (S-27, S-26) are of cuboctahedral habit with a near similar development of {111} and {100} surfaces (Fig. 2f, g). The first has a layered cuboctahedral core and mixed-habit surrounding, while the second exhibits a mixed-habit structure throughout the whole. In both cases the relative proportion of cube faces slowly increases towards the crystal periphery reflecting the inhibition of {111} layered growth. S-37 diamond of almost cubic overall shape in fact has a mixed-habit structure dominated by

{111} sectors and only minor {100} surfaces leading to negative relief at {100} positions (Fig. 2h). The S-4 sample is a typical cube with a curvilinear concentric zonation showing thin growth sectors of octahedron (Fig. 2i).

Infrared spectroscopy

The summary of the FTIR measurement results for studied diamonds are presented in Fig. 3; measured values are provided only for the zone of mixed-habit growth as a centre-to-rim profiles through neighbouring cube and octahedron growth sectors. These include total nitrogen content (N, in atomic ppm), nitrogen aggregation state (expressed as a proportion of B1-centres, %B1), absorption intensity of platelets-related band ($B2$, cm^{-1}) and the main band related to IR-active hydrogen (k_{3107} ; CH, cm^{-1}). The summary of FTIR and PL measurements are provided in Table 1.

Nitrogen systematics

The variability of nitrogen concentration of the mixed-habit domains in the studied sample group is non-surprisingly huge (mostly within 600–1500 ppm) as it includes

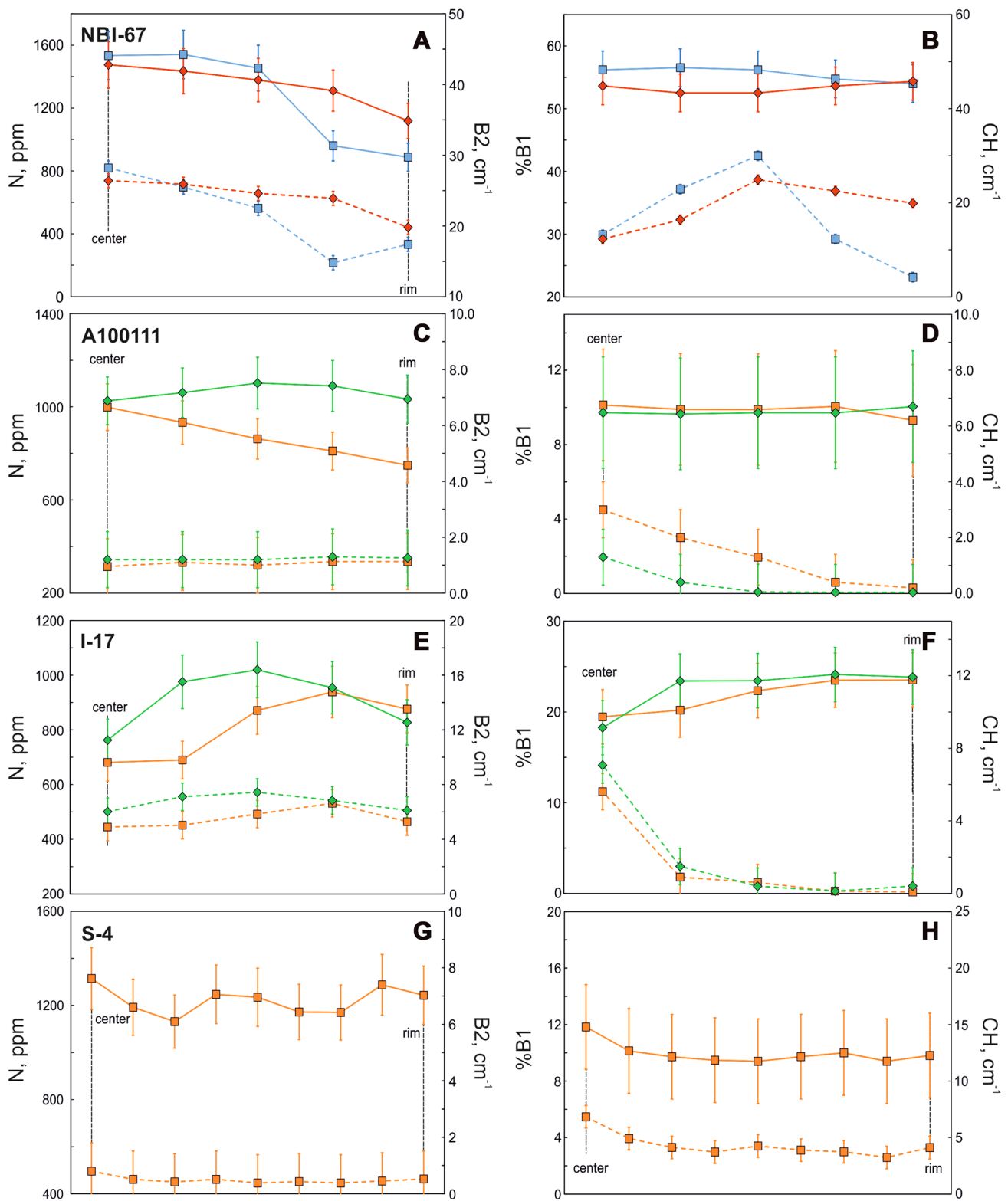


Fig. 3 Representative profiles along the octahedron and cube growth sectors of studied diamonds. *Squares* and *rhombs* correspond to values in {100} and {111} growth sectors, respectively. For the figures to the *left*, total nitrogen content (in atomic ppm) and the intensity of B2 (platelets) absorption are marked by *full* and *dashed* lines (*left* and

right Y-axes, respectively). For the figures to the *right*, nitrogen aggregation state [expressed as a proportion of B1-centres, $\%B1 = B1 / (A + B1)$] and the intensity of 3107 cm^{-1} absorption band for C–H bonding are again given by *full* and *dashed* lines and correspond to *left* and *right* Y-axes, respectively)

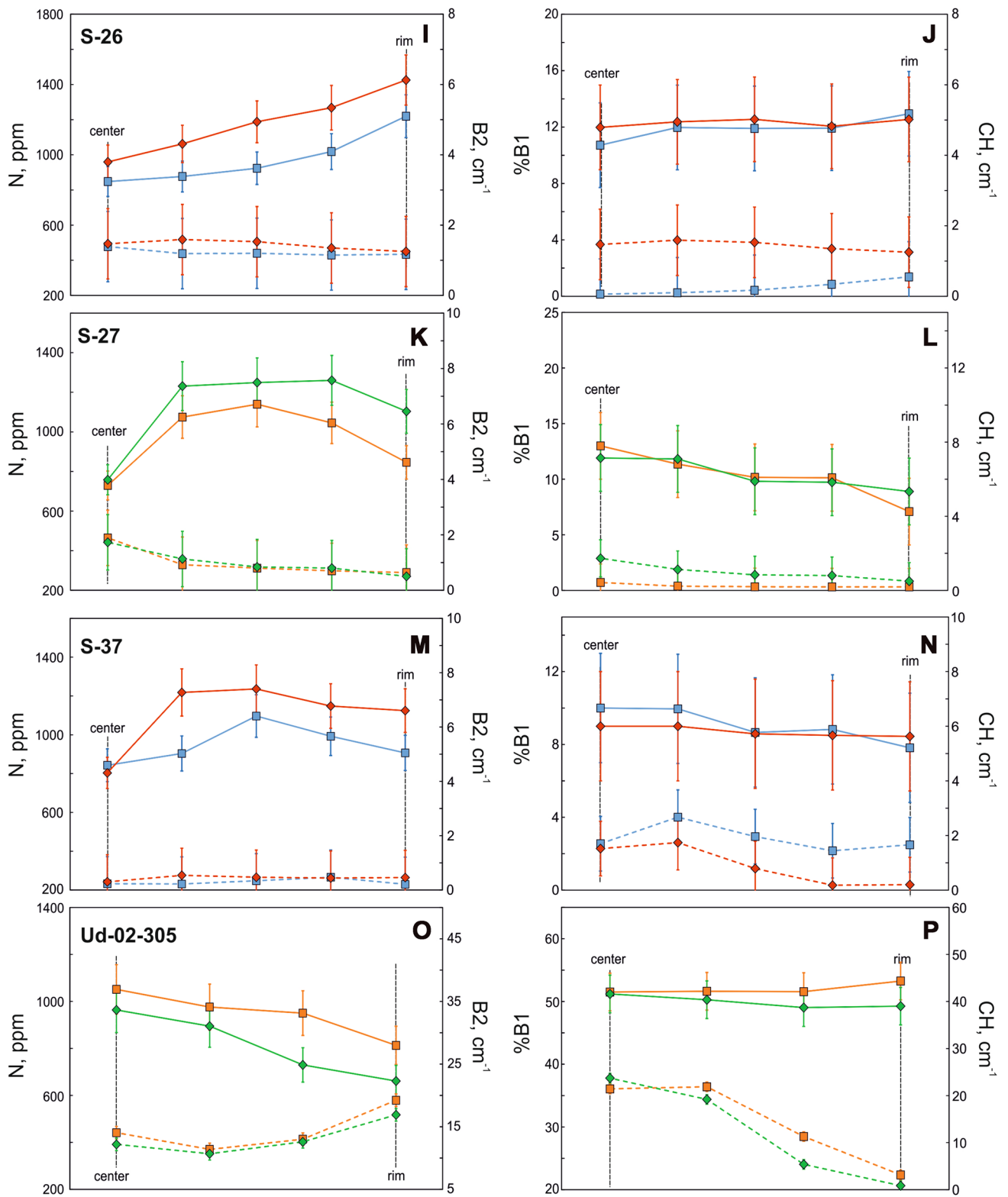


Fig. 3 continued

Table 1 Summary of the FTIR and PL characteristics of studied mixed-habit diamonds

Sample	Sector	Nitrogen content and aggregation	$\Delta_N^{111-100}$ (%)	Hydrogen absorption, k_{3107} , cm^{-1}	$\Delta_H^{111-100}$ (cm^{-1})	Additional luminescence centres
NBI-67	{100}	887–1540 ppm, 48–55% B1	−4/+27	4.2–30	+6.5/−15.7	N3, S2, 537, 573, 603.8, 621, 640, 701, 715, 725, 738, 750 and 793 nm features
A100111	{111}	1118–1475 ppm, 51–54% B1		12.3–24.9		N3 and weak 793 nm
	{100}	679–897 ppm, 9–10% B1	+9/+40	0.2–3.0	−0.2/−1.7	S3, S2, 537, 562, 603.8, 738, 752, 788 and 793 nm features
	{111}	1026–1102 ppm, 10% B1		0.0–1.3		Weak S2, 788 and 793 nm features
I-17	{100}	549–718 ppm, 19–24% B1	−6/+29	0.1–5.6	−0.2/+1.5	No PL
	{111}	763–1020 ppm, 18–24% B1		0.1–7.1		
S-4	{100}	1170–1314 ppm, 9–12% B1	n.d.	3.2–6.8	n.d.	S1, S3, S2, 537, 562, 694, 708 and 793 nm
	{111}					Weak PL bands of the same set as in {111}
S-26	{100}	848–1220 ppm, 11–13% B1	+12/+22	0.1–0.6	−0.0/−0.5	No PL
	{111}	960–1425 ppm, 12–13% B1		0.0–0.1		
S-27	{100}	729–1139 ppm, 7–13% B1	+4/+23	0.2–0.4	−0.1/−0.2	No PL
	{111}	1104–1260 ppm, 9–12% B1		0.0–0.2		
S-37	{100}	843–1097 ppm, 8–10% B1	−5/+26	1.4–2.7	+0.5/−1.5	S2, 537, 562, 793 nm
	{111}	804–1236 ppm, 8–9% B1		0.2–1.7		Weak 793 nm
Ud-02-305	{100}	813–1051 ppm, 52–53% B1	−10/−30	3.1–21.9	+2.3/−5.9	N3, S2, 537, 573, 603.8, 621, 640, 701, 715, 725, 738, 750, 788 and 793 nm features
	{111}	661–964 ppm, 49–51% B1		0.9–23.7		Similar to that in {111} but only N3 as a strong band
A1263	{100}	1194–1407 ppm, 11–12% B1	−4/−39	0.7–10.4	+2.3/−5.2	S3, S1, S2, 537, 603.8, 694, 710, 788 and 793 nm
	{111}	956–1387 ppm, 10–12% B1				Similar to that in {111} but with a weaker total intensity

Fractionation factor $\Delta_N^{111-100}$ is given in relative % and calculated as $(N_{\{111\}} - N_{\{100\}})/N_{\{111\}}$

diamonds with drastically different growth histories and represents several different kimberlitic fields. The total N content is also remarkably lower than that reported in most of comprehensive studies focused on mixed-habit diamonds (1500–2700 ppm) (Rondeau et al. 2004; Howell et al. 2013a; Smit et al. 2016). Within-crystal variations are more limited but also notable (from 80 to 500 ppm). All of the studied samples are of type IaAB (i.e. with nitrogen atoms making up A- and B1-centres of N_2 and N_4V structure, respectively) but with a relatively low nitrogen aggregation state (expressed as a proportion of B1-type defects, %B1 = $B1/(B1 + A)$) mostly within 6–12%.

The patterns of nitrogen distribution are slightly different but most of them follow one scenario based on (1)

relatively constant (A100111, NBI-67; Fig. 3a, c) or slightly increasing N content (S-27, S-37, I-17; Fig. 3e, k, m) at the initial stage of mixed-habit growth), (2) gradual decrease of the N content by 110–650 ppm (i.e. from the values close to the measurement uncertainty to statistically significant) in both {111} and {100} growth pyramids as the growth terminates (e.g. for S-27, S-37, I-17; Fig. 3e, k, m), and (3) different enrichment of the {111} sector in nitrogen relative to {100} by 80–440 ppm (9–40% relative to enriched octahedron sectors), similar to that multiply reported earlier for natural and synthetic diamonds (e.g. Burns et al. 1990; Reutsky et al. 2008; Rondeau et al. 2004; Zedgenizov and Harte 2004; Howell et al. 2013a). The A100111 diamond has the nearly constant N content (within the uncertainty)

through {111} sector but decreasing N content through a {100} sector (Fig. 3c). The {100} sector in the I-17 diamond shows a gradual N enrichment throughout the whole mixed-habit domain until it equals the N level of the {111} sector. For the internal zones of NBI-67 and A100111 diamonds, $\Delta_N^{111-100}$ factor (i.e., difference in nitrogen content between adjacent sectors of octahedron and cube) is within the analytical uncertainty and may be influenced by the signal integration with adjacent zones.

Two “hourglass” diamonds (A1263 and Ud-02-305) where the internal mixed-habit domains are overgrown by an octahedron show gradual decrease of the N content by order of 240–430 ppm. Due a specific structure of these two diamonds, it is hard to construct adequate IR profiles. However, both diamonds have octahedron sectors relatively depleted in nitrogen (by order of 80–300 ppm) that is especially obvious on the N distribution map for A1263 (Fig. 4a). The “reverse” type of fractionation with $\Delta_N^{111-100} < 0$ is unusual but has been reported for some similar diamonds from Siberian kimberlites (Bulanova et al. 2002).

The principal exception from above is the S-26 diamond that shows similar trend towards extinction of the octahedron

facets (Fig. 2g) and positive $\Delta_N^{111-100}$ of 110–260 ppm (Fig. 3i) but is characterized by a gradual increase of the N content towards the rim in both {111} and {100} sectors.

The mixed habit domain of the S-4 cubic diamond exhibits a fluctuating N content (Fig. 3g) within a relatively narrow range of 1130–1320 ppm. Due to a small scale of {111} sectors, we were not able to localize the spectrum acquisition points for S-4 cubic reliably for precise $\Delta_N^{111-100}$ estimation.

Nitrogen aggregation, platelets and calculated mantle residence conditions

Regardless of details of the mixed-habit domain structure and associated nitrogen distribution, the proportion of B1-centres (%B1) is rather similar for most of the studied diamonds (including one “hourglass” octahedron A1263) (7–13%); commonly it does not exceed the value of a few per cents for the intracrystal variations (Fig. 3, right side) that is within the analytical uncertainty and undetectable on the FTIR maps (Fig. 4c). Relatively variable (up to 4%) nitrogen aggregation degree is observed for the S-27 diamond where %B1 slightly decreases towards the crystal

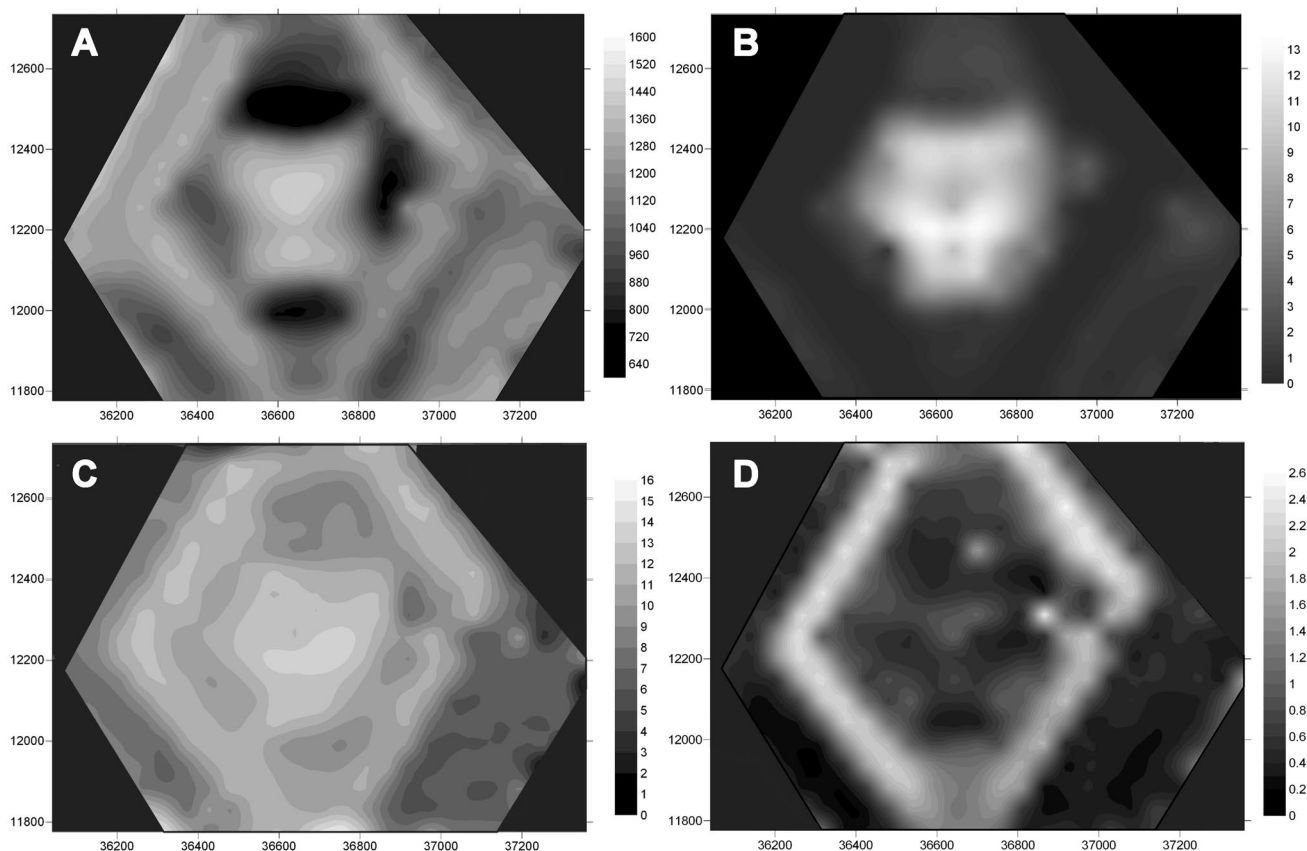


Fig. 4 FTIR maps of the A1263 octahedron showing the distribution of the total nitrogen content (**a**), values of the absorption intensity for the major hydrogen-related peak (3107 cm^{-1}) (**b**), nitrogen aggregation state (**c**) and values of the platelets absorption intensity (**d**)

periphery but still close the 2σ interval. Sample I-17 has a higher (20–24%) but still poorly variable $B1$ percentage. NBI-67 and Ud-02-305 samples have similar and prominently more aggregated nitrogen impurity (49–55% of $B1$ centres). The difference between {111} and {100} sectors for all studied diamonds is extremely low (within 0–3% $B1$) and does not seem statistically significant.

Based on the total nitrogen content and its aggregation state (Fig. 5), most of the data cluster nicely within a narrow temperature range between 1050 and 1100 °C, and also likely to have quite similar mantle residence times. The more the nitrogen converted to $B1$ -type defects (up to 23–24% in case of I-17 diamond), the higher the temperature and the longer the residence time estimates quantified (possibly up to 2 Ga at 1100 °C, with a bit younger but not “cooler” outermost zone). Two of studied diamonds (NBI-67, Ud-02-305) are strongly distinct and were possibly subjected to mantle residence at higher temperature (up to 1150 °C).

All the diamonds with a low $B1$ percentage show weak $\sim 1355\text{--}1370\text{ cm}^{-1}$ absorption attributed to $B2$ -type defect (platelets) (Woods 1986). For most of the samples the absorption intensity is too low to check for its correlation with the N content or % $B1$ proportion (Fig. 5b), though for some diamonds it does clearly correlate well with an overall nitrogen distribution (Fig. 3a, e, m). Diamonds with mixed-habit interiors overgrown by octahedrons (Ud-02-305, A1263) do not exhibit any obvious behaviour of the platelets (Figs. 3o, 4d) possibly due to partial annealing-induced degradation (Fig. 5b).

Hydrogen content

Hydrogen is well known as a common impurity in natural and synthetic diamonds (e.g. Woods and Collins 1983;

Kiflawi et al. 1996; De Weerd and Collins 2006) that has a number of typical peaks in the infrared spectrum (1405, 2785, 3050, 3107, 3154, 3236 cm^{-1}). Here, distribution of IR-active hydrogen has been evaluated using its major peak at 3107 cm^{-1} found to be related to combination of hydrogen with nitrogen and a vacancy (Goss et al. 2014). Most of the studied mixed-habit diamonds are extremely poor in the IR-active H defect (e.g. Figure 3d, j, l); the latter reaches have notable amount only in high- $B1$ diamonds NBI-67 and Ud-02-305 (Fig. 3b, p) and also in the inner zone of I-17 close to microinclusion-rich core (Fig. 3f). Hydrogen content either remains relatively constant and slightly decreases from the centre towards the rim (Fig. 3d, f, h, j, l, p) or tends to correlate with the N content (Fig. 3b, n). Growth sectors of cube are always richer in hydrogen relative to those of octahedron (Fig. 3, right side, and the H-defect distribution map in Fig. 4b), with the distribution pattern for the outer zone of NBI-67 diamond (two near-rim data-points in Fig. 3b) being quite uncertain and related to complexity of the outer growth domain.

UV fluorescence and PL spectroscopy data

Three of the diamonds (I-17, S-26 and S-27) do not exhibit a clear UV fluorescence pattern. Other six that were further studied by means of the confocal PL spectroscopy are characterized by the two distinct patterns based on the abundance of defects containing highly aggregated nitrogen and nickel (Fig. 6).

The Ud-02-305 diamond shows a uniform blue luminescence throughout the crystal except opaque whitish {100} growth sectors and the outer coat (Fig. 6a). The PL spectra of different blue-coloured zones are similar and exhibit N_3 -type centre (aggregations of three adjacent nitrogen atoms plus vacancy, N_3V) with a zero-phonon line (ZPL)

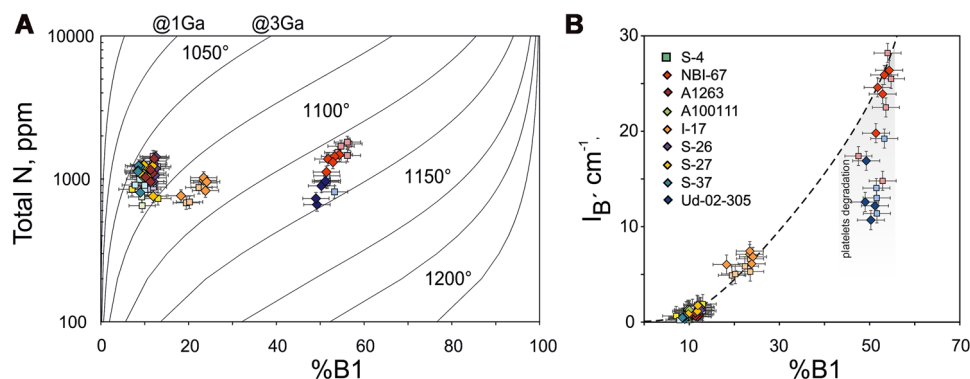


Fig. 5 Nitrogen aggregation characteristics of the studied diamonds. **a** Time–temperature integration plot for the studied mixed-habit diamonds based on the nitrogen content (Total N) and aggregation state (% $B1$). The function curves were calculated and plotted using equations from Leahy and Taylor (1997). For each temperature, *left*

and *right* isochrones are for 1 and 3 Ga residence, respectively. **b** Dependence between nitrogen aggregation state (% $B1$) and intensity of platelets' absorption (I_B). For both diagrams, *filled rhombs* mark the values for different growth zones of {111} sectors, whereas cubes nearby represent those for {100} sectors

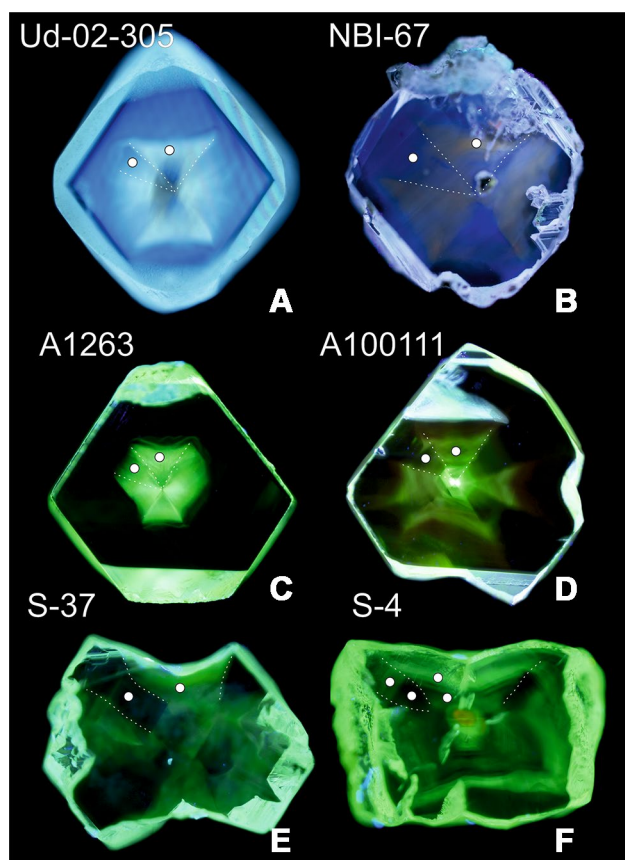


Fig. 6 Spatial distribution of UV fluorescence excited by the 532-nm laser in six diamond crystals. Points of the spectra acquisition and examined growth sectors are given

at 415 nm (Davies 1972; van Wyk 1982) (Fig. 7a). This is typical of IaAB-type diamonds with a high degree of nitrogen aggregation; it is also supported by a weak 496-nm feature related to H4 centre (B-centre plus vacancy) (Davies 1972). The central part of the diamond also shows a series of absorption features at 523, 537, 603.8, 623, 642, 700, 727, 738, 787 and 793 nm. Except of the latter two, all mentioned lines are not detected in the outer zones of the blue-coloured crystal core and have notably lower (but still detectable) intensity in {111} sectors relative to {100} (Fig. 7a). Several of the observed PL features (S2 centre with a ZPL at 523.2 nm, S3 at 496.7, and 793 nm centre) are attributed to the presence of nickel–nitrogen complexes with a nickel ion in the position of divacancy and three, two and four nitrogen atoms, respectively (analogues of NE3, NE1 and NE9 paramagnetic centres) (Yelissev and Kanda 2007). These are common in cubic crystals and cubic sectors of natural mixed-habit diamonds (Bokii et al. 1986; Welbourn et al. 1989; Lang et al. 2004). Some of the centres observed (603.8, 788 nm) typically correlate with the intensity of S2- and S3-type luminescence (Field 1992; Kupriyanov et al. 1999) and are also abundant in

cube growth sectors in natural mixed-habit diamonds (Plotnikova et al. 1980; Zaitsev 2001). Nickel-related origin is also considered for 537, 623, 642, 727 and possibly 700 nm centres (Kupriyanov et al. 1999; Nadolnny et al. 1999; Yelissev and Kanda 2007). The 737–738 nm feature is similar to that observed in Si- and Ni-containing synthetic diamonds (Kiflawi et al. 1997) but also possible due to Si–V bonding (Breeding and Wang 2008). Similar list of defects is also typical of the other diamond characterized by a high proportion of B1-defects (NBI-67) (Fig. 7c). In contrast to Ud-02-305, NBI-67 exhibits a slightly yellowish fluorescence of {100} growth sectors (Fig. 6c) that is consistent with a lower intensity of N3-centre luminescence relative to Ni-bearing defects mentioned above (Fig. 7c).

Although the other four diamonds (S-4, S-37, A100111, A1263) have distinct growth structures, their UV fluorescence patterns are similar and show green coloration of {100} growth pyramids and non-fluorescent {111} sectors (Fig. 6b, d–f). According to the characteristic PL spectra, the colour is induced by a series of nickel-bearing centres preferentially incorporated into {100} growth sectors (e.g. Welbourn et al. 1989; Lang et al. 2004; Howell et al. 2013a, 2015; Smit et al. 2016 and references therein) (Fig. 7b, d–f). The luminescent core of the A1263 diamond (Fig. 6b) shows PL features of S3, S1, S2, 537, 603.8, 788, 793, 694 and 710 nm (Fig. 7b); the last two were also found to contain nickel ions (Nadolnny et al. 1999). Despite the light greenish luminescence {111} growth sectors exhibit much lower intensity of mentioned PL features, but the list of those is similar for {111} and {100}. The similar set of defects was detected in A100111 sample (S3, S2, 537, 562, 575, 603.8, 710, 738, 752, 788, 793 nm) (Fig. 7d), though for S-37 and S-4 this is more limited (S2, 537, 562 and 793 nm for the former; S3, S1, S2, 537, 562, 694, 708 and 793 nm for the latter) (Fig. 7e, f). According to the recent review of Dischler (2012), 694, 701 and 793 nm features for all four studied diamonds with the mentioned fluorescence pattern may be due to S5 and S9 centres also bearing nickel atoms along with a nitrogen-vacancy combinations.

Discussion

Nitrogen and hydrogen systematics of the mixed-habit diamonds

Summary of the present data is given schematically in Fig. 8 along with the data for natural mixed-habit diamonds published earlier. As compared to the nitrogen systematics for previously studied natural samples (Fig. 8a), inclusion-free mixed-habit samples from the present work are evidently poorer in nitrogen (mostly within 800–1300 vs 1500–2700 ppm and exhibit an variable $\Delta_N^{111-100}$ value

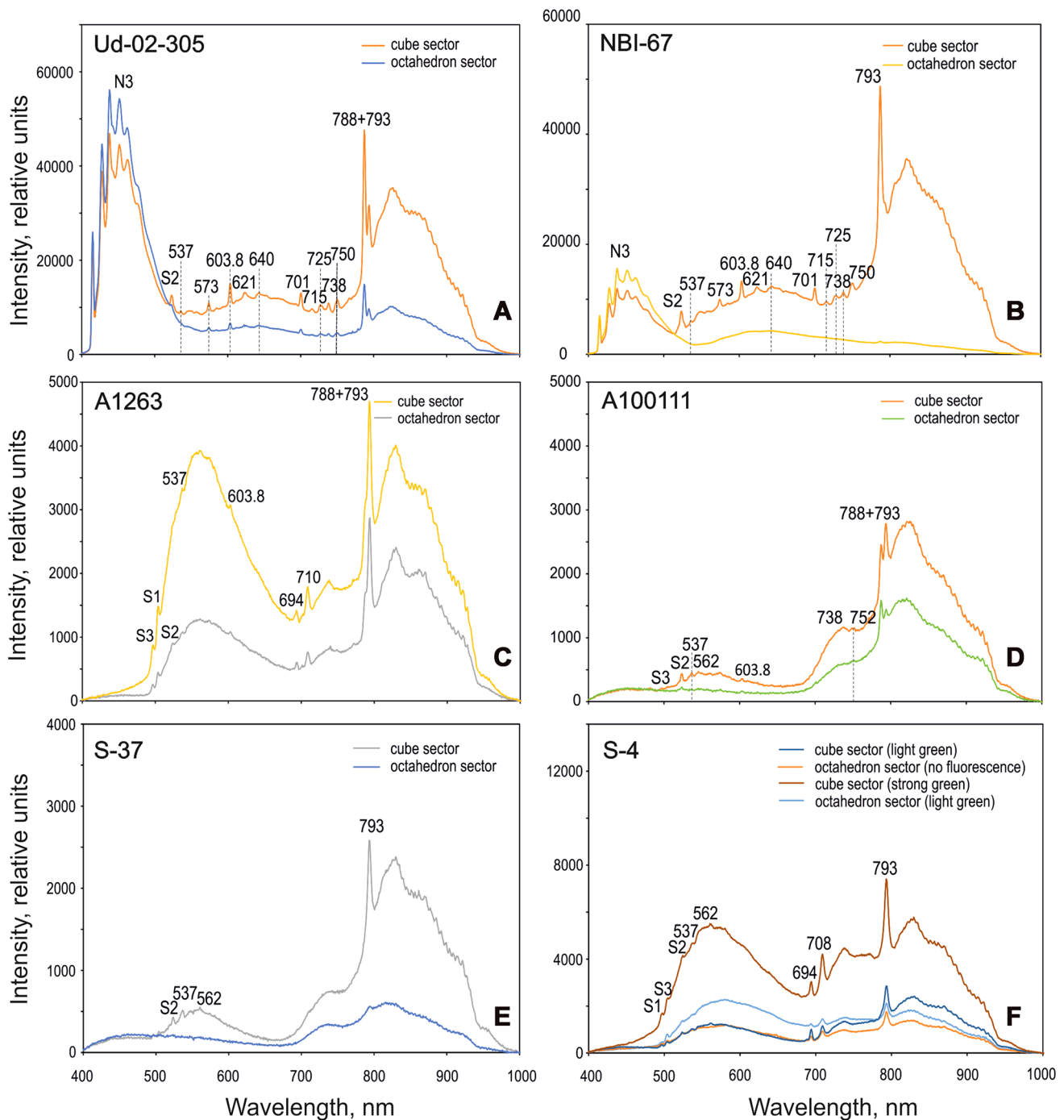


Fig. 7 Photoluminescence spectra acquired at 77 K through the excitation with 375 nm picosecond laser in the growth sectors of cube and octahedron of studied diamonds

from 40% of that in the enriched $\{111\}$ sector to totally negligible. Evidently, no principal difference in the type of $\Delta_N^{111-100}$ fractionation are observed for those growth zones in the studied diamonds that show clearly positive $\Delta_N^{111-100}$ factors and the N-rich mixed-habit diamonds reported earlier, for which the N content was estimated by means of FTIR and varied from more than 40% to within-uncertainty

scale (Fig. 8a). In contrast to majority of the diamonds studied here, samples reported by Howell et al. (2013a) and Smit et al. (2016) exhibit a wide range of mantle residence parameters (as follows from %B1 values). Additionally, two “hourglass” diamonds (A1263, Ud-02-305) show unusual nitrogen partitioning into the $\{100\}$ sectors ($\Delta_N^{111-100}$ well below zero) similar to that observed by Bulanova et al.

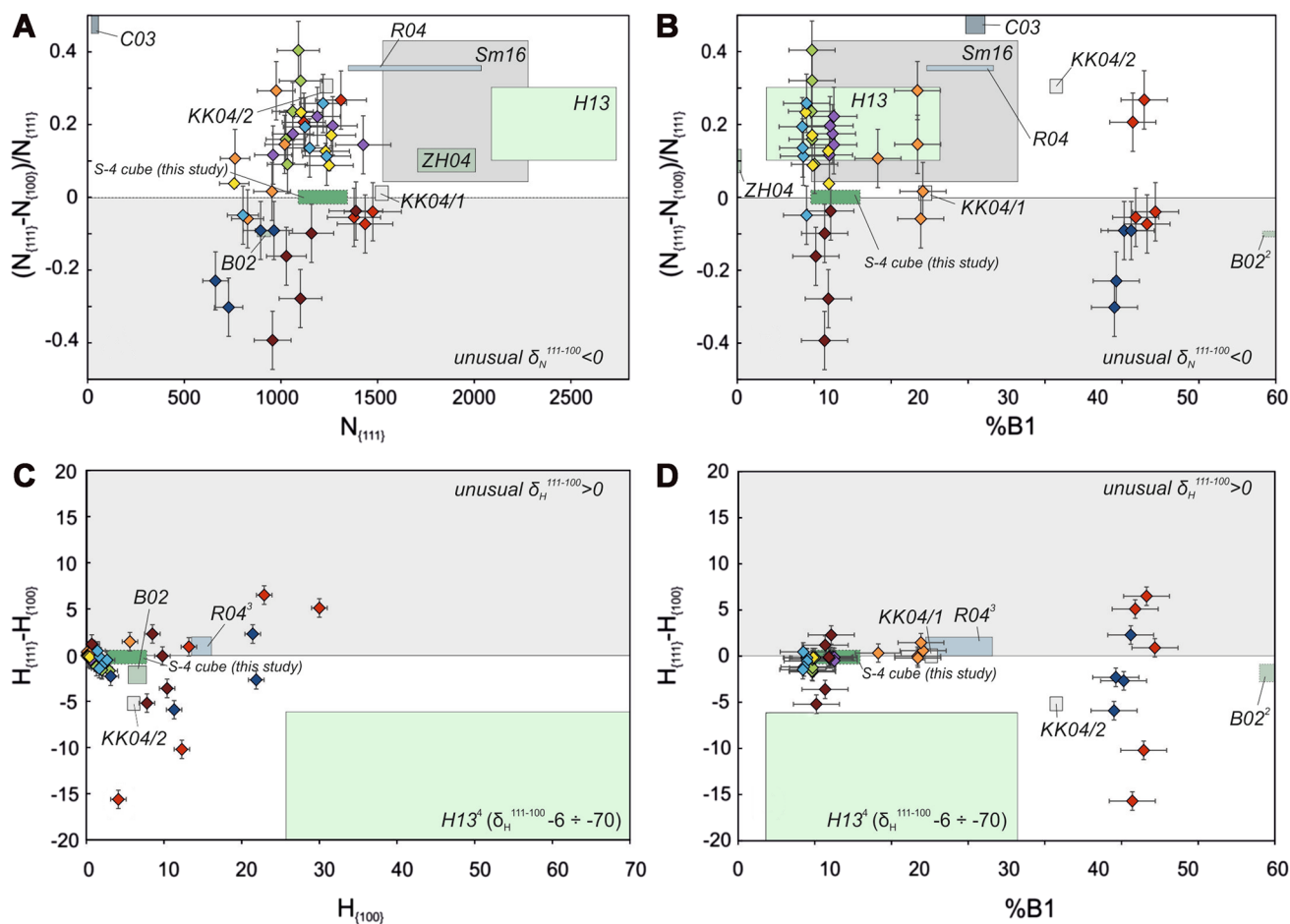


Fig. 8 Co-variation of major impurity characteristics (nitrogen content, aggregation state, intensity of hydrogen-related IR-absorption along with partitioning values of N and H) in studied diamonds and mixed-habit diamonds reported earlier (see references and discussion in the text). The legend follows that of Fig. 5. Abbreviations for the literature data for mixed-habit diamonds here are: *Sl6* 13 N-rich diamonds from Marange, Zimbabwe (Smit et al. 2016), *R04* 2 N-rich diamonds from unknown source (Rondeau et al. 2004); *H13* 13 N-H-rich diamonds from unknown source (Howell et al. 2013a); *ZH04* cuboctahedron from the Udachnaya pipe (Zedgenizov and Harte 2004); *KK04/1* mixed-habit dodecahedron from the Northern Urals placer (Kaminsky and Khachatryan 2004); *C03* low-N diamond from

Wellington, New South Wales (Cartigny et al. 2003); high-*B1* octahedron from the Udachnaya pipe (Kaminsky and Khachatryan 2004); *B02* high-*B1* octahedron from the Mir pipe (Bulanova et al. 2002). *Superscript 1* Relative position for the S-4 cubic diamond is shown as we were unable to localize the spectra acquisition point precisely in a thin {111} sector, and no information on the {111}/{100} partitioning is available. *Superscript 2* Relative position is given for the figurative rectangle of the Mir diamond reported by Bulanova et al. (2002) as the real %B1 values exceed 90%. *Superscript 3* The used values from Rondeau et al. (2004) are for 1405 cm^{-1} . *Superscript 4* Only the upper limit is given for the H partitioning reported by Howell et al. (2013a)

2002; more specifically, a trend of {100} N enrichment towards the N-poorer zones is observed. The two diamonds have different %B1, high (Ud-02-305) and low (A1263), and corresponding PL luminescence patterns dominated by aggregated nitrogen (N3) and nickel-nitrogen centres, respectively. Another diamond with the high percentage of B1 centres (NBI-67) does not differ in the type of nitrogen distribution ($\Delta_N^{111-100} > 0$) from majority of low-*B1* diamonds (Fig. 8a) with a common green Ni-related or no even PL luminescence that suggests similar nitrogen partitioning at drastically different temperatures or times of mantle residence and corresponding defect-producing

annealing. Together with the absence of any signatures typical for vacancy-producing events that might enhance the impurity re-distribution (e.g. plastic deformation or irradiation), such as H3, H4 or 575 nm PL features, the data reject any possibility of annealing-caused nitrogen redistribution and support the idea of growth-controlled nitrogen behaviour (discussed below). As green luminescence induced by nitrogen-nickel defects in diamonds is commonly (e.g. Howell et al. 2013a) but not necessarily linked with a peridotitic suite for diamond growth (e.g. Smit et al. 2016 and references therein), its absence in diamonds S-26 and S-27 with $N_{\text{tot}}\text{-}\%B1$ values (and, thus, annealing parameters)

similar to most of the other studied samples is likely indicative of the low-Ni, possibly eclogitic environment. Since no transitions and almost no absorption intensity changes had been experimentally observed for nickel-related defects at typical growth temperatures for lithospheric diamonds (1300–1600 °C) (Yelissev and Kanda 2007), the abundance of defects with only high N/Ni (e.g. S5 or S9) in studied diamonds of cubic (S4) and near-cubic habit (S-37) may a sensitive indicator of either a lower-Ni environment or lower growth rate (Kanda and Lawson 1995; Kiflawi et al. 2002).

Unlike most of thoroughly studied populations of mixed-habit diamonds (e.g. Howell et al. 2013a) and numerous reports for cubic and coated diamonds, the intensity of hydrogen-related absorption in almost gem-quality transparent cube sectors in the diamonds studied here (with a typical nickel-related luminescence and %B1 values within only 13%) lies within a few cm^{-1} (see diamonds A100111, S-4, S-26, S-27, S-37; Fig. 3d, h, j, l, n). A higher mantle residence temperature and/or—less likely—longer period at the similar nitrogen content observed for the I-17 diamond (Fig. 5) leads to %B1 increase up to 25%, but does not produce any significant changes in hydrogen absorption (that is still low) or hydrogen partitioning (almost negligible within uncertainties of the method). As the B1 value remains nearly constant throughout a mixed-habit domain of this diamond pointing out single-act growth and further annealing, the higher hydrogen absorption in the crystal centre may reflect gradual depletion of the parental fluid by hydrogen towards growth termination (Fig. 3f). For all mentioned diamonds with a relatively low IR-active hydrogen content a $\Delta_{\text{H}}^{111-100}$ is near-zero (and so less precisely estimated) (Fig. 8) and shifts towards a “normal” negative values only in a bit hydrogen-enriched zones of A1263 sample. As the hydrogen concentrations are of trace levels and should not affect the partitioning, we may suggest that for the low %B1 and low H diamonds a pattern of hydrogen distribution might not be constrained good enough due to the method limitations. More ambiguous is a hydrogen behaviour in natural diamonds with progressively aggregated nitrogen as deduced from the two samples here (NBI-67, Ud-02-305) and some literature data for high-%B1 octahedral diamonds (Bulanova et al. 2002; Kaminsky and Khachatryan 2004) (Fig. 8). Two of the high-%B1 diamonds studied here have relatively high hydrogen absorption at 3107 cm^{-1} ($10\text{--}30 \text{ cm}^{-1}$). While the Ud-02-305 sample has the predominant partitioning of hydrogen into {100} sectors similar to that observed in the high-B1 octahedron by Bulanova et al. (2002) and association of H with N impurity throughout the both crystal (Fig. 3o, p), inner zones the NBI-67 diamond lack this correlation (likely due to a complex and unclear structure of the internal zones) and outer zones show H enrichment of

{111} sectors (i.e. unusual $\Delta_{\text{H}}^{111-100}$ partitioning) (Fig. 3a, b). The reason for the latter is not evident. According to studies of Saguy et al. (2003) and Shiryaev et al. (2007), diffusion of hydrogen in a growing diamond may be successfully controlled by other matrix impurities, including nitrogen. The latter, if presented in a diamond as A-defects, may significantly enhance H diffusion through its loss in the annealing process and $A \rightarrow B1$ transformation due to a weak N–H interaction relative to that between H and single nitrogen (C-type) defects (Shiryaev et al. 2007). This might cause a partial re-distribution that might result in uneven distribution of hydrogen within growth sectors, and hence would account for the mismatch in the $\Delta_{\text{H}}^{111-100}$ with the commonly observed values.

Growth morphology, impurity systematics and growth conditions of mixed-habit diamonds

At the dawn of growth theories the morphology of a growing crystal was related to either atomic bonding forces or distinct growth mechanisms depending on the saturation value (Sunagawa 1984). In case of a diamond, the latter is favoured by distinct growth patterns and impurity and isotope characteristics of cubic and octahedral crystals, but appears to be controversial when applied to samples with a mixed-habit history where distinct growth pyramids occur at exactly the same thermodynamic state and composition of the system. In fact, growth sector zoning is likely to occur in crystals grown at high rates (e.g. Paterson and Stephens 1992; Northrup and Reeder 1994) that makes such growth strongly kinetics-dependent and a priori may almost preclude the application of equilibrium-based theories and calculations. Some models based on slow lattice diffusion of incompatible components (e.g. Watson and Liang 1995; Watson 1996) favour a possibility of low growth rate for some magmatic and metamorphic environments, but their application to diamonds grown from high-PT high-density fluids or melts seems questionable. Nonetheless, at low growth rates fractionation of impurities based on the match of their size with the different distances between the dangling bonds in different crystallographic directions may have an equilibrium character and thus may shift from the equilibrium via (1) the change of growth rate and/or (2) change of impurity speciation (and atomic size) in the parental media.

There is a limited agreement in the nitrogen content and partitioning between growth sectors of a diamond if one compares the data from nature and experiments. In addition to distinct bulk chemistries, i.e. metal–carbon systems for the most of synthetic diamonds (e.g., Palyanov et al. 2010, 2013) and generally carbonatitic and carbonate–silicate high-density fluids for natural Siberian diamonds (e.g., Zedgenizov et al. 2009; Skuzovatov et al. 2011, 2016),

diamonds with contrasting nitrogen contents are produced in these environments, in most cases not higher than 200–300 ppm for synthetic diamonds grown in metal–carbon systems (without special N-containing additives) versus up to a few thousands ppm for kimberlitic diamonds (Evans 1992; Cartigny et al. 2004; Mikhail and Howell 2016). Some non-metallic systems (see “Introduction” in Palyanov et al. 2010) including those compositionally similar to the natural ones (e.g., Palyanov et al. 2007) and even some metal–carbon systems (Borzdov et al. 2002; Palyanov et al. 2010) are known so far to successfully produce nitrogen-rich diamonds (up to 3300 ppm) but to reach these levels of the impurity content within the stability of a monocrystalline diamond required up to unexpected 0.2 atomic % of N in the parental melts. More uniform are the data for the nitrogen partitioning between growth sectors. The early experimental studies on the diamond growth in metal–carbon systems followed by some more recent works on diamond synthetics showed the 2–4 times enrichment in N content of {111} growth pyramids relative to {100} (Boyd et al. 1988; Burns et al. 1990; Reutsky et al. 2008; Babich and Feigelson 2009a, b). Smaller but still notable partitioning of the nitrogen impurity between growth sectors was observed in some individual natural diamonds (Zedgenizov and Harte 2004; Howell et al. 2013a; Smit et al. 2016; this study). This is not only the case of nitrogen but also some important trace elements, e.g. Ni that tends to partition into the {100} growth sectors as a Ni–N-containing defects in natural diamonds (Lang et al. 2004; Howell et al. 2013a, b; Smit et al. 2016; this study) due to different surface characteristics of the {100} sectors in natural diamonds and their synthetic analogues. This similarity in the nitrogen incorporation should reflect a single reason for the selective impurity uptake, i.e. generally similar nitrogen incorporation dependent of distinct atomic surface structure of cube and octahedron diamond surfaces and kinetics- and/or growth-rate control of the impurity incorporation during mineral growth (Watson and Liang 1995; Watson 1996).

For nitrogen, the principal differences between synthetic diamonds and most of natural diamonds are as follows: (1) the difference in the {100} surface features (microscopically coarse, unknown but most probably atomically coarse or even blocky for the most of natural diamonds; microscopically flat in case of synthetic diamonds) that may lead to different character in $\Delta_N^{111-100}$ fractionation, and (2) different residence times at HP-HT conditions and resulting aggregation state of nitrogen in a diamond. During residence at mantle conditions nitrogen commonly tends to form larger aggregates through interaction with available vacancies (as in NV or B1 centres) (Allen and Evans 1981; Evans and Qi 1982; Pinto et al. 2012; Jones et al. 2015) rather than re-distribute between growth sectors due to numerous dislocations at sector boundaries

separating the adjacent growth pyramids (Chernov et al. 1980). Thus, for nitrogen-poor synthetic diamonds grown in relatively short periods without a subsequent annealing, only the first factor really affects nitrogen partitioning, and the positive $\Delta_N^{111-100}$ partitioning demonstrated by these diamonds (Boyd et al. 1988; Burns et al. 1990; Reutsky et al. 2008; Babich and Feigelson 2009a) should reflect the “ideal” model driven by the surface crystal chemistry even at low levels of N content. The difference in {100} surface configuration between natural and synthetic diamonds evidently does not affect N partitioning but may effectively influence that of other mentioned impurities, like hydrogen (e.g., systematic H enrichment of octahedral sectors in IIb diamonds; Shiryayev et al. 2007) or nickel ({111} Ni enrichment in synthetic samples; Collins et al. 1990).

For natural diamonds, positive $\Delta_N^{111-100}$ partitioning is well documented only for samples with high N (Howell et al. 2013a; Smit et al. 2016), whereas the only N-poor mixed-habit diamond with a positive $\Delta_N^{111-100}$ fractionation factor (Cartigny et al. 2003) has been interpreted by Howell et al. (2015) as actually non-mixed-habit (Fig. 8a). For most the diamonds studied here, we observe similar trends of {111} nitrogen enrichment that is for some extent shadowed by the analytical uncertainties but at the lower N content in a diamond that may result from either in the parental composition (that might be poorer in nitrogen), or different behaviour of the impurity. Nitrogen distribution profiles suggest that growth likely occurred in a closed system gradually depleted in nitrogen (in case of its compatible behaviour relative to a diamond) or at slowly decreasing growth rate leading to a decreasing kinetics-dependent incorporation of an impurity (if nitrogen behaves as incompatible). Some diamonds exhibit a clear nitrogen depletion at the initial stage of growth because a portion of nitrogen was consumed for nickel–nitrogen defects and growth proceeded at a bit higher temperature (Kanda and Lawson 1995). As compared to the experiments that modelled diamond morphology change through the increase of impurity content in the parental melt (e.g., Palyanov et al. 2010, 2013), a scale to which the nitrogen content changes during a natural single-stage diamond growth (e.g. in this study) is very limited and, therefore, unable to affect the stability of distinct growth shapes but more likely is a function of growth conditions. According to experimental growth and impurity distribution of mixed-habit diamonds (Reutsky et al. 2008; Babich and Feigelson 2009a), nitrogen content in a diamond may be directly dependent on the growth rate that is consistent with a incompatible behaviour of nitrogen relative to a growing diamond (e.g. Boyd et al. 1994; Cartigny et al. 2001). The two conclusions that may be drawn from this are the following: (1) high overall growth rate would result in a shift from equilibrium fractionation leading to saturation of the more defective cube surface

with the incompatible impurity (as in case of “hourglass” diamonds studied here and by Bulanova et al. 2002), (2) a slight decrease in the overall growth rate towards the crystal periphery would lead to the nitrogen fractionation close to “equilibrium” as supported by most of the remaining diamonds (e.g., NBI-67, A100111, S-27, S-37). The missing point here is a definition of the actually high and low growth rates as natural diamonds grown at definitely high rates are believed to exhibit fibrous patterns with numerous microinclusions (e.g. Zedgenizov et al. 2009; Skuzovatov et al. 2016) and should contain more nitrogen than their inclusion-free analogues if accepting the incompatible nature of nitrogen. However, for a series of the Botswanian diamonds, Smit et al. (2016) reported a usual positive type of the $\Delta_N^{111-100}$ partitioning but with surprisingly higher level of $\Delta_N^{111-100}$ if considering inclusion-free {100} sectors (hence likely grown at relatively low growth rates) as compared to {100} sectors rich with numerous methane inclusions that should reflect high growth rates. The mechanism for these variations needs an additional clarification.

Hydrogen impurity and its distribution within diamond crystals in relation to growth parameters is much more difficult matter, as the ratio de-facto hydrogen content and hydrogen-related IR-absorption is unclear and cannot be assessed quantitatively (e.g. as highlighted by Sweeney et al. 1999). It has been also a matter of long-term discussions whether IR-active hydrogen is structurally bonded, e.g. with nitrogen-related defects (Rondeau et al. 2004) or present on a surface of cavities/microinclusions (Woods and Collins 1983) or some sort of macroscopically detected “disc-crack-like” defects (Walmsley et al. 1987; Howell et al. 2013a). Possible role of microinclusions in enhancing hydrogen-related absorption is especially emphasized in cloudy diamonds where the maximum intensity of the corresponding spectral features usually associates with inclusion-rich cubic cores (e.g. Skuzovatov et al. 2011, 2015, 2016). The mixed-habit domains of the diamonds studied here are evidently macrodefect- and inclusion-free, whereas a mixed-habit structure is observed only through CL/PL excitation. Thus we may reliably regard the observed IR hydrogen absorption as structure-related and presenting at least a significant portion of a total hydrogen or even a whole amount of that.

Based on a number of direct observations, the enrichment of cubic diamonds in hydrogen and a strong partitioning of the impurity to cube growth sectors of mixed-habit samples are known (e.g. Suzuki and Lang 1976; Woods and Collins 1983; Howell et al. 2013a and references therein). According to some recent models, this tends to reflect a necessity of high hydrogen content in the parental fluid/melt required for cubic diamond growth (e.g. Rondeau et al. 2004; Howell et al. 2013a). Strongly contradicting standpoint is met when looking up a clear correlation of

3107 cm^{-1} and other hydrogen-related IR features with diamond annealing and nitrogen aggregation process (Kiflawi et al. 1996; De Weerd and Kupriyanov 2002; Goss 2003; De Weerd and Collins 2006) as well as an extreme enrichment in hydrogen of some high-%B1 octahedral diamonds (Jakoubovskii and Adriaenssens 2002). In general, we may conclude that both low-B1 diamonds with low amount of IR-active hydrogen and high-B1 octahedrons with more complex growth history may resemble a similar and common type of negative $\Delta_H^{111-100}$ partitioning that should reflect “normal” lattice-controlled hydrogen distribution. If assuming the reports of high-B1 (from 29 up to 100%) mixed-habit octahedra with a much lower hydrogen absorption (Bulanova et al. 2002; Kaminsky and Khachatryan 2004) and strongly hydrogen-enriched mixed-habit samples with “normal” $\Delta_H^{111-100}$ partitioning at relatively low %B1 (mostly within 15%) (Howell et al. 2013a), we may suggest that diamond mixed-growth may occur not only from hydrogen-rich media (Howell et al. 2013a) but also from fluids/melts with drastically different H contents or at different conditions directly affecting the kinetics of hydrogen incorporation.

Conclusions

A significant variability of spectroscopic features for a series of mixed-habit diamonds directly indicates the diversity of growth conditions may be generated. Definitely grown at relatively constant pressure–temperature and closed or nearly closed system conditions, mixed-habit stones though exhibit different degree of impurity partitioning possibly linked to variable degree of non-equilibrium controlled directly by growth kinetics and temperature. Based on this study, we may argue that mixed-habit diamond growth is successfully reproduced in natural systems with a lower impurity content as compared to some recent conclusions considering only N-rich diamonds and—thus—nitrogen-rich fluids/melts. Relatively constant and notable partitioning of impurities between adjacent growth sectors reported earlier for a series of mixed-habit diamonds seems to result from a better analytical sensitivity at much higher nitrogen content, since the high nitrogen content itself could not produce larger $\Delta_N^{111-100}$ fractionation values. A similar pattern is typical of hydrogen behaviour, but in contrast to nitrogen this impurity may be partially re-distributed during post-crystallization annealing and formation of A- and B1-type defects. Significantly lower content of IR-active hydrogen in some samples studied here relative to “standard” sectorial diamonds with cubic sectors enriched with that impurity, shift the lower limit of H concentration towards extremely depleted. The combined data on relatively low nitrogen and low IR-active hydrogen content may suggest

that diamond-forming systems are not necessary to contain high concentrations of these impurities for mixed-habit growth to be reproduced. The crucial role for this as well as for unusual impurity fractionation between growth sectors may be in the overall growth rate which affects the total impurity content in a diamond, and relative growth rates of {111} and {100} sectors that—in case of a prominent difference—may shift the $\Delta_N^{111-100}$ partitioning towards cuboid enrichment. The detection of abundant Ni–N defects and their absence in diamonds with similar impurity contents and mantle residence conditions may also extend a field of possible geochemical affinities for growth of mixed-habit diamonds to low-Ni or maybe even Ni-free environments, such as pyroxenitic or eclogitic suites.

Acknowledgements The manuscript has benefited significantly from critical reviews of the two anonymous referees, editorial remarks of Max Schmidt and personal communication from Vadim Reutsky. This study was supported by the Russian Science Foundation (Grant No. 16-17-10067).

References

- Allen BP, Evans T (1981) Aggregation of nitrogen in diamond, including platelet formation. *Proc R Soc Lond A* 375:93–104
- Babich YV, Feigelson BN (2009a) Spatial distribution of the nitrogen defects in synthetic diamond monocrystals: data of IR mapping. *Geochem Int* 47(1):94–98
- Babich YV, Feigelson BN (2009b) Distribution of N+ centers in synthetic diamond single crystals. *Inorg Mater* 45(6):616–619
- Bokii GB, Bezrukov GN, Klyuev YuA, Naletov AM, Nepsha VI (1986) Natural and synthetic diamonds. Nauka, Moscow (**in Russian**)
- Borzdov M, Pal'yanov Y, Kupriyanov I, Gusev V, Khokhryakov A, Sokol A, Efremov A (2002) HPHT synthesis of diamond with high nitrogen content from an Fe₃N–C system. *Diam Relat Mater* 11:1863–1870
- Boyd SR, Pillinger CT, Milledge HJ, Mendelsohn MJ, Seal M (1988) Fractionation of nitrogen isotopes in a synthetic diamond of mixed crystal habit. *Nature* 331:604–607
- Boyd SR, Pineau F, Javoy M (1994) Modeling the growth of natural diamonds. *Chem Geol* 116:29–42
- Boyd SR, Kiflawi I, Woods GS (1995) Infrared absorption by the B nitrogen aggregate in diamond. *Philos Mag B* 72:351–361
- Breeding CM, Wang W (2008) Occurrence of the Si–V defect center in natural colorless gem diamonds. *Diam Relat Mater* 17(7–10):1335–1344
- Bulanova GP, Barashkov YuP, Talnikova SB, Smelova GB (1993) Natural diamond—genetic aspects. Nauka, Novosibirsk (**in Russian**)
- Bulanova GP, Pearson DG, Hauri EH, Griffin BJ (2002) Carbon and nitrogen isotope systematics within a sector-growth diamond from the Mir kimberlite, Yakutia. *Chem Geol* 188:105–123
- Burns RC, Cvetkovic V, Dodge CN, Evans DJF, Rooney M-LT, Spear PM, Welbourn CM (1990) Growth-sector dependence of optical features in large synthetic diamonds. *J Cryst Growth* 104:257–279
- Cartigny P, Harris JW, Javoy M (2001) Diamond genesis, mantle fractionations and mantle nitrogen content: a study of $\delta^{13}\text{C-N}$ concentrations in diamonds. *Earth Planet Sci Lett* 185:85–98
- Cartigny P, Harris JW, Taylor A, Davies R, Javoy M (2003) On the possibility of a kinetic fractionation of nitrogen stable isotopes during natural diamond growth. *Geochim Cosmochim Acta* 67(8):1571–1576
- Cartigny P, Stachel T, Harris JW, Javoy M (2004) Constraining diamond metasomatic growth using C- and N-stable isotopes: examples from Namibia. *Lithos* 77:359–373
- Chernov AA, Givargizov EI, Bagdasarov KhS, Kuznetsov VA, Dem'yanets LN, Lobachev AN (1980) Current state of crystallography, vol 3. Nauka, Moscow (**in Russian**)
- Collins AT, Kanda H, Burns RC (1990) The segregation of nickel-related optical centers in the octahedral sectors of synthetic diamond. *Philos Mag B* 61(5):797–810
- Davies G (1972) The effect of nitrogen impurity on the annealing of radiation damage in diamond. *J Phys C* 5(17):2534–2542
- De Weerd F, Collins AT (2006) Optical study of the annealing behaviour of the 3107 cm⁻¹ defect in natural diamonds. *Diam Relat Mater* 15:593–596
- De Weerd F, Kupriyanov I (2002) Report on the influence of HPHT annealing on the 3107 cm⁻¹ hydrogen related absorption peak in natural type Ia diamonds. *Diam Relat Mater* 11:714–715
- Dischler B (2012) Handbook of spectral lines in diamond. Springer, Berlin
- Evans T (1992) Aggregation of nitrogen in diamond. In: Field JE (ed) The properties of natural and synthetic diamond. Academic Press, London, pp 259–290
- Evans T, Qi Z (1982) The kinetics of the aggregation of nitrogen atoms in diamond. *Proc R Soc A* 381:169–178
- Field JE (1992) The properties of natural and synthetic diamond. Academic Press, London
- Goss JP (2003) Theory of hydrogen in diamonds. *J Phys Condens Matter* 15:R551–R580
- Goss JP, Briddon PR, Hill V, Jones R, Rayson MJ (2014) Identification of the structure of the 3107 cm⁻¹ H-related defect in diamond. *J Phys Condens Matter* 26:145801
- Haggerty SE (1986) Diamond genesis in a multiply-constrained model. *Nature* 320:34–38
- Harrison EL, Tolansky S (1964) Growth history of a natural octahedral diamond. *Proc R Soc Lond A* 279:490–496
- Howell D, Griffin WL, Piazzolo S, Say JM, Stern RA, Stachel T, Nasdala L, Rabeau JR, Pearson NJ, O'Reilly SY (2013a) A spectroscopic and carbon-isotope study of mixed-habit diamonds: impurity characteristics and growth environment. *Am Miner* 98(1):66–77
- Howell D, Griffin WL, Pearson NJ, Powell W, Wieland P, O'Reilly SY (2013b) Trace element partitioning in mixed-habit diamonds. *Chem Geol* 355:134–143
- Howell D, Stern RA, Griffin WL, Southworth R, Mikhail S, Stachel T (2015) Nitrogen isotope systematics and origins of mixed-habit diamonds. *Geochim Cosmochim Acta* 157:1–12
- Iakubovskii K, Adriaenssens GJ (2002) Optical characterization of natural Argyle diamonds. *Diam Relat Mater* 11(1):125–131
- Jones R, Goss JP, Pinto H, Palmer DW (2015) Diffusion of nitrogen in diamond and the formation of A-centers. *Diam Relat Mater* 53:35–39
- Kaminsky FV, Khachatryan GK (2004) The relationship between the distribution of nitrogen impurity centres in diamond crystals and their internal structure and mechanism of growth. *Lithos* 77:255–271
- Kanda H, Lawson SC (1995) Growth temperature effects of impurities in HP/HT diamonds. *Ind Diam Rev* 55(2):56–61
- Khokhryakov AF, Sokol AG, Borzdov YM, Palyanov YM (2015) Morphology of diamond crystals grown in magnesium-based systems at high temperatures and high pressures. *J Cryst Growth* 426:276–282

- Kiflawi I, Fisher D, Kanda H, Sittas G (1996) The creation of the 3107 cm^{-1} hydrogen absorption peak in synthetic diamond single crystals. *Diam Relat Mater* 5:1516–1518
- Kiflawi I, Sittas G, Kanda H, Fisher D (1997) The irradiation and annealing of Si-doped diamond single crystals. *Diam Relat Mater* 6(1):146–148
- Kiflawi I, Kanda H, Lawson SC (2002) The effect of the growth rate on the concentration of N and transition metals impurities in HPHT diamonds. *Diam Relat Mater* 11:204–211
- Kupriyanov IN, Gusev VA, Borzdov YuM, Kalinin AA, Pal'yanov N (1999) Photoluminescence study of annealed nickel- and nitrogen-containing synthetic diamond. *Diam Relat Mater* 8(7):1301–1309
- Lang AR (1974) Glimpses into the growth history of natural diamonds. *J Cryst Growth* 24–25:108–115
- Lang AR, Yelissev AP, Pokhilenko NP, Steeds JW, Wotherspoon A (2004) Is dispersed nickel in natural diamonds associated with cuboid growth sectors in diamonds that exhibit a history of mixed-habit growth? *J Cryst Growth* 263:575–589
- Lang AR, Bulanova GP, Furkert S, Fisher D, Sarua A (2007) Defects in a mixed-habit Yakutian diamond: studies by optical and cathodoluminescence microscopy, infrared absorption, Raman scattering and photoluminescence spectroscopy. *J Cryst Growth* 309:170–180
- Leahy K, Taylor WR (1997) The influence of the Glennie domain deep structure on the diamonds in Saskatchewan kimberlites. *Russ Geol Geophys* 38(2):481–491
- Mikhail S, Howell D (2016) A petrological assessment of a diamonds as a recorder of the mantle nitrogen cycle. *Am Miner* 101:780–787
- Moore M, Lang AR (1972) On the internal structure of natural diamond of cubic habit. *Philos Mag* 26(6):1313–1325
- Nadolinniy VA, Yelissev AP, Baker JM, Newton ME, Twitchen DJ, Lawson SC, Yuryeva OP, Feigelson BN (1999) A study of ^{13}C hyperfine structure in the EPR of nickel-nitrogen-containing centres in diamond and correlation with their optical properties. *J Phys Condens Matter* 11:7357–7376
- Northrup PA, Reeder RJ (1994) Evidence for the importance of growth-surface structure to trace element incorporation in topaz. *Am J Sci* 79:1167–1175
- Orlov YL (1977) *The mineralogy of the diamond*. Wiley, New York
- Palyanov YN, Borzdov YM, Bataleva YV, Sokol AG, Palyanova GA, Kupriyanov IN (2007) Reducing role of sulfides and diamond formation in the Earth's mantle. *Earth Planet Sci Lett* 260:242–256
- Palyanov YN, Borzdov YM, Khohryakov AF, Kupriyanov IN, Sokol AG (2010) Effect of nitrogen impurity on diamond crystal growth processes. *Cryst Growth Des* 10:3169–3175
- Palyanov YN, Khokhryakov AF, Borzdov YM, Kupriyanov IN (2013) Diamond growth and morphology under the influence of impurity adsorption. *Cryst Growth Des* 13(12):5411–5419
- Paterson BA, Stephens WE (1992) Kinetically-induced compositional zoning in titanite: implications for accessory-phase/melt partitioning of trace elements. *Contrib Mineral Petrol* 109:373–385
- Pinto H, Jones R, Palmer DW, Goss JP, Briddon PR, Öberg S (2012) On the diffusion of NV defects in diamond. *Phys Status Solidi A* 209(9):1765–1768
- Plotnikova SP, Klyuev YA, Parfianovich KA (1980) Long-wave photoluminescence of natural diamonds. *Miner Zh* 2(4):75–80 (in Russian)
- Reutsky VN, Harte B, Borzdov YM, Palyanov YN (2008) Monitoring diamond crystal growth, a combined experimental and SIMS study. *Eur J Miner* 20:365–374
- Rondeau B, Fritsch E, Guiraud M, Chalain JP, Notari F (2004) Three historical 'asteriated' hydrogen-rich diamonds: growth history and sector-dependent impurity incorporation. *Diam Relat Mater* 13:1658–1673
- Saguy C, Cytermann C, Fizgeer B, Richter V, Avigal Y, Moriya N, Kalish R, Mathieu B, Deneuille A (2003) Diffusion of hydrogen in undoped, p-type and n-type doped diamonds. *Diam Relat Mater* 12:623–631
- Seal M (1965) Structure in diamonds as revealed by etching. *Am Miner* 50:105–123
- Shiryaev AA, Grambole D, Rivera A, Herrmann F (2007) On the interaction of molecular hydrogen with diamonds: an experimental study using nuclear probes and thermal desorption. *Diam Relat Mater* 16:1479–1485
- Skuzovatov SY, Zedgenizov DA, Shatsky VS, Ragozin AL, Kuper KE (2011) Composition of cloudy microinclusions in octahedral diamonds from the Internatsional'naya kimberlite pipe (Yakutia). *Russ Geol Geophys* 52(1):85–96
- Skuzovatov SY, Zedgenizov DA, Ragozin AL, Shatsky VS (2012) Growth medium composition of coated diamonds from the Sytykanskaya kimberlite pipe (Yakutia). *Russ Geol Geophys* 53(11):1197–1208
- Skuzovatov SY, Zedgenizov DA, Rakevich AL, Shatsky VS, Martynovich EF (2015) Multiple growth events in diamonds with cloudy microinclusions from the Mir kimberlite pipe: evidence from the systematics of optically active defects. *Russ Geol Geophys* 56(1–2):330–343
- Skuzovatov SY, Zedgenizov DA, Howell D, Griffin WL (2016) Various growth environments of cloudy diamonds from the Malobotuobia kimberlite field (Siberian craton). *Lithos* 265:96–107
- Smit KV, Shirey SB, Stern RA, Steele A, Wang W (2016) Diamond growth from C–H–N–O recycled fluids in the lithosphere: evidence from CH_4 micro-inclusions and $\delta^{13}\text{C}$ – $\delta^{15}\text{N}$ – $\delta^{15}\text{N}$ content in Marange mixed-habit diamonds. *Lithos* 265:68–81
- Sunagawa I (1984) Morphology of natural and synthetic diamond crystals. In: Sunagawa I (ed) *Materials science of the earth's interior*. Terra Science Publications, Tokyo/D Reidel, Dordrecht, pp 303–330
- Sunagawa I (1990) Growth and morphology of diamond crystals under stable and metastable conditions. *J Cryst Growth* 99:1156–1161
- Suzuki S, Lang AR (1976) Internal structures of natural diamond crystals revealing mixed-habit growth. In: Daniel P (ed) *Diamond research*. Industrial Diamond Information Bureau, Ascot, England, pp 39–47
- Sweeney RJ, Prozesky VM, Viljoen KS, Connell S (1999) The sensitive determination of H in diamond by infrared (FTIR) spectroscopy and microelastic-recoil (u-ERDA) techniques. *Nucl Instrum Methods Phys Res B* 158:582–587
- Van Wyk JA (1982) Carbon-13 hyperfine interaction of the unique carbon of the P2 (ESR) or N3 (optical) centre in diamond. *J Phys C Solid State Phys* 15:L981–L983
- Walmsley JC, Lang AR, Rooney M-LT, Welbourn CM (1987) Newly observed microscopic planar defects on [111] in natural diamond. *Philos Mag Lett* 55:209–213
- Watson EB (1996) Surface enrichment and trace element uptake during crystal growth. *Geochimica et Cosmochimica Acta* 60(24):5013–5020
- Watson EB, Liang Y (1995) A simple model for sector zoning in slowly grown crystals: implications for growth rate and lattice diffusion, with emphasis on accessory minerals in crustal rocks. *Am Miner* 80(11–12):1179–1187
- Welbourn CM, Rooney M-LT, Evans DJF (1989) A study from diamonds of cube and cube related shape from the Jwaneng mine. *J Cryst Growth* 94:229–252
- Woods GS (1986) Platelets and the infrared absorption of type Ia diamonds. *Proc R Soc Lond A* 407:219–238

- Woods GS, Collins AT (1983) Infrared absorption spectra of hydrogen complex in type I diamonds. *J Phys Chem Solids* 44:471–475
- Yelisseyev A, Kanda H (2007) Optical centers related to 3d transition metals in diamond. *New Diam Front Carbon Technol* 17(3):127–178
- Zaitsev AM (2001) *Optical properties of diamond: a data handbook*. Springer, Berlin
- Zedgenizov DA, Harte B (2004) Microscale variations of $\delta^{13}\text{C}$ and N content within a natural diamond with mixed-habit growth. *Chem Geol* 205:169–175
- Zedgenizov DA, Harte B, Shatsky VS, Politov AA, Rylov GM, Sobolev NV (2006) Directional chemical variations in diamonds showing octahedral following cuboid growth. *Contrib Miner Petrol* 151:45–57
- Zedgenizov DA, Ragozin AL, Shatsky VS, Araujo D, Griffin WL, Kagi H (2009) Mg and Fe-rich carbonate silicate high-density fluids in cuboid diamonds from the Internationalnaya kimberlite pipe (Yakutia). *Lithos* 112:638–647